HHS Public Access

Author manuscript

*Nat Chem Biol*. Author manuscript; available in PMC 2010 November 01.

Published in final edited form as:

*Nat Chem Biol*. 2010 May ; 6(5): 369–375. doi:10.1038/nchembio.349.

# Electro-chemical coupling in the voltage-dependent phosphatase Ci-VSP

**Susy C. Kohout**[1], **Sarah C. Bell**[2], **Lijun Liu**[3], **Qiang Xu**[3], **Daniel L. Minor Jr.**[3,4,5,7], and **Ehud Y. Isacoff**[1,2,6,7,8,#]

[1]Department of Molecular and Cell Biology, University of California, Berkeley, CA 94720

[2]Chemical Biology Graduate Program, University of California, Berkeley, CA 94720

[3]Cardiovascular Research Institute, University of California, San Francisco, California 94158

[4]Departments of Biochemistry and Biophysics, and Cellular and Molecular Pharmacology, University of California, San Francisco, California 94158

[5]California Institute for Quantitative Biosciences, University of California, San Francisco, California 94158

[6]Helen Wills Neuroscience Institute, University of California, Berkeley, CA 94720

[7]Physical Biosciences Division, Lawrence Berkeley National Laboratory, Berkeley, CA 94720

[8]Material Science Division, Lawrence Berkeley National Laboratory, Berkeley, CA 94720

## Abstract

In the voltage sensing phosphatase, Ci-VSP, a voltage sensing domain (VSD) controls a lipid phosphatase domain (PD). The mechanism by which the domains are allosterically coupled is not well understood. Using an *in vivo* assay, we find that the inter-domain linker that connects the VSD to the PD is essential for coupling the full-length protein. Biochemical assays show that the linker is also needed for activity in the isolated PD. We identify a late step of VSD motion in the full-length protein that depends on the linker. Strikingly, this VSD motion is found to require $PI(4,5)P_2$, a substrate of Ci-VSP. These results suggest that the voltage-driven motion of the VSD turns the enzyme on by rearranging the linker into an activated conformation, and that this activated conformation is stabilized by $PI(4,5)P_2$. We propose that Ci-VSP activity is self-limited because its decrease of $PI(4,5)P_2$ levels decouples the VSD from the enzyme.



[#]Corresponding author: ehud@berkeley.edu.

**Author Contributions**

S.C.K. designed, conducted and analyzed the VCF experiments and the confocal experiment, as well as conducted and analyzed the malachite green assay and the CD spectroscopy and wrote the paper. S.C.B. designed, conducted and analyzed the *in vivo* activity assay and edited the paper. L.L. expressed and purified the cytosolic domain proteins and edited the paper. Q.X. helped design the malachite green assay as well as expressed and purified the cytosolic domain proteins. D.L.M. designed and initiated the CD spectroscopy as well as edited the paper. E.Y.I. designed the VCF experiments as well as the *in vivo* activity assay and wrote the paper.

**Competing financial interests statement**

The authors declare no competing financial interests.

## Introduction

The *Ciona intestinalis* voltage-sensing phosphatase, Ci-VSP, has an N-terminal domain that resembles the voltage sensing domain (VSD) of voltage-gated ion channels and a C-terminal domain that is homologous to the "phosphatase and tensin homologue deleted on chromosome 10" (PTEN) protein, a lipid and protein phosphatase1–3 (Fig. 1a). Ci-VSP is the first member of the voltage dependent family of proteins that is not an ion channel. Instead, Ci-VSP takes an electrical signal in the form of membrane potential and converts it to a chemical signal through its phosphatase activity. Its discovery has raised questions about how a membrane-spanning sensor domain can couple to both the gates of ion channel pore domains and to a cytoplasmic enzyme. For voltage-gated potassium channels, the linker between S4 in the VSD and S5 in the pore domain has been shown to be necessary for coupling the voltage sensing to the gating of the pore 4–6.

The homology between the Ci-VSP phosphatase domain (PD) and PTEN led to the discovery that Ci-VSP is a voltage-dependent lipid phosphatase1. Although PTEN dephosphorylates the 3-phosphate of phosphatidylinositol 3,4,5-trisphosphate ($PI(3,4,5)P_3$), Ci-VSP has been shown to remove the 5-phosphate of both $PI(3,4,5)P_3$, dephosphorylating it to phosphatidylinositol 3,4-bisphosphate ($PI(3,4)P_2$), and phosphatidylinositol 4,5-bisphosphate ($PI(4,5)P_2$), dephosphorylating it to phosphatidylinositol 4-phosphate (PI(4)P)7–9. While there are sequence divergences between Ci-VSP and PTEN, there are a number of notable similarities. The catalytic domains are 44% identical, and the residues that are known to be important for catalysis are highly conserved. They share several basic amino acids just upstream of the catalytic domain, which are known as the "$PI(4,5)P_2$ binding motif" (PBM) in PTEN10. In PTEN, the PBM is essential for membrane targeting and this has been attributed to an interaction between $PI(4,5)P_2$ and the basic residues in the PBM11–14. The homologous region in Ci-VSP links the VSD to the PD (Fig. 1a), suggesting that it may couple voltage sensing to enzymatic activity, analogous to the function of the S4–S5 linker in $K^+$ channels.

A major unresolved question about Ci-VSP, and its homologues from sea squirt to vertebrates, is how do the voltage-driven structural rearrangements of the VSD control the activity of the enzyme? Mutations in the VSD-PD linker have been shown to eliminate activity,1,15 suggesting either that this linker plays a direct role in the function of the PD or that it is important for coupling the VSD to the PD. To gain insight into this issue, we examined the activity of linker mutants in the isolated PD of the protein *in vitro*. We found that point mutations substantially reduce activity and that a linker deletion ablates activity altogether. These observations indicate that the linker has a direct role in enzymatic function. Because mutations in the linker directly affect the activity of the enzyme domain, activity cannot be used to determine if the mutants also affect coupling. We therefore developed an alternative coupling assay using Voltage Clamp Fluorometry (VCF)16,17. The assay is based on recent evidence that manipulation of the phosphatase by mutation of the catalytic cysteine 363 to a serine or by an active site blocker alters the gating current (also known as "sensing current")18. This alteration demonstrates that inter-domain coupling between the PD and the VSD of the protein can be detected optically as an influence of PD mutants on VSD motion as measured by VCF15,17,19. Because the effect of the C363S

mutation is modest, we searched for another phosphatase mutation that has a bigger impact on the VSD.

Using VCF to measure the voltage-driven motion of the VSD, we identified a new a catalytic site mutation, D331A, which strongly alters the voltage dependence and kinetics of VSD motion and, thus, provides a high accuracy gauge of inter-domain coupling. With this measure of coupling, we find that mutations in the VSD-PD linker compromise coupling. These linker mutants are also found to alter a late step of VSD motion. Strikingly, we find that $PI(4,5)P_2$ modulates both coupling and the late VSD motion. We propose a model where $PI(4,5)P_2$ interacts with the linker to stabilize an enzyme-activating conformation induced by the depolarization-driven motion of the VSD. The modulation by the substrate could provide a mechanism for enhancing enzymatic activity when $PI(4,5)P_2$ is high and reducing activity when it is low to limit the degree of $PI(4,5)P_2$ depletion.

## Results

### Effect of mutations in VSD-PD linker on activity

Ci-VSP has an N-terminal VSD and a C-terminal PD that are connected by a 16 amino acid linker (Fig. 1a). To understand how the voltage-driven motions of the VSD are coupled to the activity of the PD, we examined the linker, which shares 50% identity with the PTEN N-terminal (PBM) (Fig. 1b, top). The PTEN PBM contains several basic amino acids, including K13 and R15, which have been found to be mutated in cancer cells20–22. K13E disrupts the membrane targeting of PTEN, even though the active site is still capable of catalysis12. These functionally important PTEN residues lie in the second half of the PBM and are conserved in Ci-VSP's VSD-PD linker as K252 (PTEN K13) and R254 (PTEN R15) (Fig. 1b, top). A recent study showed that the double mutation of R254A with its neighbor R253A eliminates voltage-dependent changes in activity, leading to the proposal that they serve as a part of a PBM and an inter-domain coupler for Ci-VSP15.

We focused on three consecutive residues, K252, R253 and R254 in Ci-VSP (Fig. 1b, top), and made individual glutamine mutations to neutralize the charge carried by each position. These mutations were made in the background of G214C, which served as a fluorophore labeling site. Because the level of activity will depend on both the rate of catalysis by each molecule of Ci-VSP and on the number of Ci-VSP molecules in the plasma membrane, it was important to determine if the mutations affect expression level. We assessed the expression level of the three mutants following labeling of the G214C position with the fluorescent probe, tetramethylrhodamine maleimide (TMRM). We found that the resting G214C-TMRM (G214C*) oocyte fluorescence at the holding potential of −80 mV (an index of the number of labeled Ci-VSP proteins on the cell surface) was as high in the three mutants (*i.e.* they expressed as well) as in wild type (Supplementary Results, Supp. Fig. 1), enabling a straightforward comparison of their activity. To measure catalytic activity, we employed a previously established assay that uses an IRK1 channel that is mutated (R228Q) to reduce $PI(4,5)P_2$ affinity1,17 (see Materials and Methods & Supp. Fig. 2). We found that K252Q and R254Q reduce voltage-dependent changes in activity to undetectable levels, and that R253Q reduces this activity by 80 ± 6% (n=8) relative to G214C* alone (Fig. 1c).

The loss of activity in the linker neutralization mutations could be due to a loss of coupling. Alternatively, it could reflect a direct effect of the mutations on the PD. To distinguish between these possibilities, we examined the effect of the K252Q, R253Q and R254Q mutations on the activity of the isolated PD construct (amino acids 240–576) *in vitro*. Circular dichroism (CD) measurements showed that the three mutant proteins were all well folded (Supp. Fig. 3). Using the malachite green activity assay to monitor phosphatase activity of the purified proteins1,8, we found that R253Q retained wild type levels of activity, but that K252Q and R254Q had reduced activity (Fig. 1d, Supplemental Methods). These *in vitro* experiments indicate that two of the three conserved basic residues have a direct influence on PD activity.

To examine the function of the Ci-VSP linker further, we carried out the malachite green *in vitro* activity assay on a PD construct from which the linker was deleted (*i.e.* where the construct begins at amino acid 256, but is otherwise wild type in sequence). This construct was well folded (Supp. Fig. 3) but completely lacked activity towards either a membrane bound PI(3,4,5)$P_3$ substrate or a water soluble inositol-(1,3,4,5)-trisphosphate ($IP_4$) substrate (Fig. 1d, Supp. Fig. 4 ). An equivalent deletion in PTEN lost activity with the membrane bound PI(3,4,5)$P_2$ but retained activity against the soluble $IP_4$ 11, distinguishing Ci-VSP from PTEN. Thus, the Ci-VSP linker is necessary for the catalytic function of the PD. These results suggest that in the full-length construct negative voltages may disable the linker, and that depolarization may allow it to assume the activating conformation that it has in the VSD-less construct in solution.

## Catalytic domain influence over the VSD

The direct effects of the linker on enzyme activity, which we observed above, mean that in order to gauge VSD-PD coupling in the full-length protein, one needs an assay that does not depend on phosphatase activity. Recently in the zebrafish VSP18, the serine mutant at the catalytic cysteine (analogous to Ci-VSP C363S) and an active site blocker, orthovanadate, were both shown to alter the “sensing” current—the analog of the gating current of voltage-gated channels. Those results imply that changes in the catalytic site influence VSD motion and that they could provide a readout of inter-domain coupling. We therefore turned next to examining the impact of catalytic site mutations on VSD motion, as measured using VCF.

We made mutations in the PD of Ci-VSP at residues that are conserved in PTEN and required for catalysis (Fig. 1b, bottom). In addition to the C363S mutation of the catalytic cysteine, which was already described1,7, we tested D331A, whose homologous mutation in PTEN (D92A) also ablates activity13,23,24. The mutations were made in the G214C fluorophore labeling site background, as was done above with the linker mutations. These catalytic mutants were fluorescently labeled to the same degree as wild type, indicating equivalent expression (Supp. Fig. 1). Although they expressed as well as wild type, C363S and D331A had no detectable voltage-dependent changes in enzymatic activity (Fig. 1c).

To probe the activity of these mutants further, we purified the isolated linker-PD construct for each mutant and tested for activity *in vitro*. CD measurements indicated that the C363S and D331A were well folded and similar to wild type (Supp. Fig. 3). The enzymatic activity was abolished in C363S and reduced by 73 ± 8% in D331A (Fig. 1d). The *in vivo* and *in*

*vitro* data agree with earlier observations on C363S in the wild type background1,7 and show that D331A also interferes with activity.

We used VCF to measure the kinetics and voltage dependence of the structural rearrangements of the VSD by monitoring the fluorescence of the TMRM attached to position G214 (G214C*) at the outer end of S4. We found that both C363S and D331A slowed the repolarization-driven motion of S4 ($\Delta F_{OFF}$) (Fig. 2a). The mutants also increased the steepness of the fluorescence-voltage (F-V) relation and shifted its midpoint in the negative direction (Fig. 2b, Supp. Table 1). D331A had the stronger effects, negatively shifting the midpoint of the F-V by 47 ± 1 mV and slowing the first component of the $\Delta F_{OFF}$ by 13 ± 1 fold. The homologous mutation in PTEN to Ci-VSP's D331A (PTEN D92A) can trap the substrate25, consistent with what appears to be stabilization by D331A of the activated state in Ci-VSP. This large influence of the catalytic site D331A mutation on VSD motion provided us with a clear report of VSD-PD coupling *in vivo* (Fig. 2c).

## Role of the VSD-PD linker in coupling

We tested the notion that the linker plays a role in coupling VSD motion to the function of the phosphatase by asking if the linker mutations weaken the influence of the catalytic site D331A mutation on the motion of the VSD. We first examined the effect on S4 motion of each of the three linker neutralizations on its own. We found that the G214C* $\Delta F_{OFF}$ and F-V of K252Q and R253Q were similar to those of wild type and that the $\Delta F_{OFF}$ and F-V of R254Q were mildly perturbed (Supp. Fig. 5, Supp. Table 1).

We next examined the effect of the linker mutants on the VSD perturbations caused by the catalytic site mutations. We found that K252Q eliminated the influence of the D331A catalytic site mutation on the VSD, ablating both the slowing of the $\Delta F_{OFF}$ (Fig. 3a) and the negative shift of the F-V (Fig. 3b, Supp. Table 1). The R253Q mutant had similar but less complete effects, reducing but not eliminating the slowing of the $\Delta F_{OFF}$ (Supp. Fig. 6a) and negative shift of the F-V (Supp. Fig. 6b, Supp. Table 1) caused by the D331A mutation. The incomplete uncoupling by R253Q is consistent with its incomplete reduction of voltage dependent enzyme activity (Fig. 1c). These results show that the linker couples the voltage-dependent structural state of the VSD to the functional state of the catalytic site in the PD.

## Role of VSD-PD linker in late step VSD motion

Having found that the conserved basic residues in the C-terminal end of the VSD-PD linker are important for coupling, we next endeavored to identify the VSD motion(s) in which the linker participates. To do this, we turned to another TMRM labeling site, Q208C, in the middle of the S3–S4 loop, where we had shown earlier that fluorescence reports on a series of voltage-driven rearrangements17 (Fig. 4a). Steps from the holding potential of −80 mV to voltages of between −150 and zero mV evoked fast and monotonic ΔFs, while more positive voltages of up to +100 mV evoked an additional slower component that decreased fluorescence. Even more positive steps, from +100 up to +200 mV, evoked yet an additional component of slow fluorescence increase (Fig. 4a).

Linker neutralization mutations K252Q, R253Q and R254Q were introduced individually into the Q208C background and their effect on the fluorescence report of TMRM (Q208C*) was tested. While the $\Delta F_{ON}$ and $\Delta F_{OFF}$ of Q208C* were unaffected by the mutations over the negative voltage range and in the lower end of the positive voltage range, all three of the mutations attenuated the amplitude of the late upward $\Delta F_{ON}$ component evoked by the largest depolarizations (Fig. 4b–d, Supp. Fig. 7a) and shifted its voltage dependence in the positive direction (Fig. 4e–h, Supp. Fig. 7b, Supp. Table 1). Thus, the linker specifically plays a role in the late step of VSD motion.

## Regulation of VSD motion by $PI(4,5)P_2$

Considering that the Ci-VSP VSD-PD linker is homologous to the N-terminal $PI(4,5)P_2$ binding domain (PBM) of PTEN, we wondered if $PI(4,5)P_2$ might modulate the function of the VSD-PD linker. To test this possibility, we set out to manipulate the concentration of $PI(4,5)P_2$ in the membrane and determine the effect on the VSD rearrangements which involve the linker according to our above results. We co-expressed Ci-VSP with the serotonin 2C receptor (5HT2C), a G-protein coupled receptor which activates phospholipase C (PLC), leading to the cleavage of a phosphodiester bond of $PI(4,5)P_2$ into diacyl glycerol (DAG) and inositol-(1,4,5)-trisphosphate ($IP_3$)26. We first tested the ability of serotonin to activate the 5HT2C receptor and deplete $PI(4,5)P_2$ in oocyte membranes by using IRK1Q as a $PI(4,5)P_2$ sensor, as shown above (Fig. 1c). We found that 10 μM serotonin evoked a reliable reduction of IRK1Q current over a time-course of 5 min (Supp. Fig. 8a). We therefore chose this time-point for our analysis.

The 5HT2C receptor was co-expressed with either the catalytically active G214C*, or the catalytically compromised G214C*/D331A. F-Vs were obtained before and 5 minutes after exposure to 10 μM serotonin. Successful activation of PLC was monitored by measuring current through the oocyte's endogenous $Ca^{2+}$ dependent $Cl^-$ channels (Supp. Fig. 9a), which are activated by the $IP_3$-induced release of $Ca^{2+}$ from internal stores. Both in the catalytically active and catalytically compromised versions of Ci-VSP, the F-V relations were shifted in the positive direction and became shallower following the addition of serotonin (Fig. 5a, Supp. Fig. 9b, Supp. Table 2). This shift could also be monitored as a decrease in fluorescence amplitude in response to a step to 0 mV following the addition of the serotonin (Supp. Fig. 9c). Another metabotropic receptor known to activate the PLC pathway, mGluR1, had the same effect (Supp. Fig. 6d, e). The similar effects of activation of the PLC-coupled 5HT2C and mGluR1 receptors indicates that Ci-VSP is modulated either by the depletion of $PI(4,5)P_2$ or by the production of $IP_3$ or DAG by PLC.

To distinguish between the possibilities that Ci-VSP is modulated either by the depletion of $PI(4,5)P_2$ or by the production of $IP_3$ or DAG, we chose an alternative method for reducing $PI(4,5)P_2$ in the membrane, which would not produce $IP_3$ or DAG. For these experiments, we employed an inducible phosphatase that hydrolyzes $PI(4,5)P_2$ into PI(4)P, thus avoiding the $IP_3$ and DAG signaling cascades27,28. The phosphatase, Inp54p, is a truncated version of a yeast inositol polyphosphate 5-phosphatase that specifically cleaves $PI(4,5)P_2$ at the 5-phosphate27. The activity of Inp54p can be triggered by the application of the small, membrane permeable organic molecule rapamycin, thereby permitting VCF measurements

of VSD motion to be made before and after $PI(4,5)P_2$ depletion. To make the Inp54p inducible by rapamycin, it was fused with one of two protein domains which heterodimerize upon addition of rapamycin: FKBP (FK506 binding protein) fused to CFP, which enables the membrane localization of the phosphatase to be visualized, and which is referred to as CFInp27. The partner protein domain, FRB (the rapamycin binding fragment of mTOR), was fused to the plasma membrane targeted Lyn N-terminal sequence (LDR)27. Previous studies have shown that rapamycin brings CFInp to the plasma membrane and reduces $PI(4,5)P_2$ concentrations in oocytes29. We confirmed that the rapamycin system was functional, finding it to efficiently shuttle the CFInp to the plasma membrane (Supp. Fig. 10a, b) and to decrease IRK1Q current (Supp. Fig. 8b).

Activation of the rapamycin system shifted the F-V to the right and decreased the slope of the F-V both in the catalytically active G214C* and in the catalytically compromised G214C*/D331A (Fig. 5b, Supp. Fig. 11a, Supp. Table 3). An enzyme-dead version of the CFInp (CFInp D281A) was mobilized to the plasma membrane by rapamycin just as well as was the wild type CFInp (Supp. Fig. 10a, b), but did not affect the F-V (Supp. Fig. 10c), indicating that the shift in the F-V is specific to $PI(4,5)P_2$ depletion.

Taken together, the similar shifts in the F-V induced by activation of the two PLC coupled GPCRs, 5HT2C and mGluR1, and the rapamycin system that dephosphorylates $PI(4,5)P_2$ to another product, demonstrate that $PI(4,5)P_2$ depletion alters the voltage-driven rearrangement of the VSD.

### $PI(4,5)P_2$ and linker mutants alter late VSD motion

The above results showed that membrane $PI(4,5)P_2$ regulates VSD motion. We next tried to identify the step of VSD motion that is affected by $PI(4,5)P_2$. For this purpose we turned once again to the TMRM labeling site Q208C, whose fluorescence reports on several distinct phases of VSD motion. We found that, in wild type Q208C*, the rapamycin depletion of $PI(4,5)P_2$ decreases the amplitude of the late step of VSD motion that is activated by depolarization to > +100 mV and shifts the voltage dependence of this component to the right (Fig. 5c, Supp. Fig. 11b, Supp. Table 3).

The effect of $PI(4,5)P_2$ depletion on the late phase of VSD motion was remarkably similar to the effect of the mutation of the basic residues in the VSD-PD linker (compare Fig. 4e-h to Fig. 5c, and Fig. 4a–d to Supp. Fig. 11b). This similarity led us to ask if $PI(4,5)P_2$ modulation actually depends on the basic residues in the linker. To test this, we co-expressed the 5HT2C receptor with the catalytically active G214C*/K252Q or the catalytically compromised G214C*/D331A/K252Q. We found that, in contrast to the wild type linker (Fig. 5a, Supp. Fig. 9b), the serotonin induced $PI(4,5)P_2$ depletion effect was absent in the K252Q linker mutant (Fig. 5d, Supp. Fig. 12a, Supp. Table 3). We also tested the rapamycin system in the catalytically compromised G214C*/D331A protein and obtained a similar result: the $PI(4,5)P_2$ depletion effect, present in the wild type linker (Fig. 5b), was absent in the K252Q linker mutant (Fig. 5e, Supp. Table 3).

Because G214C* does not clearly resolve the various components of VSD motion, we also tested the effect of $PI(4,5)P_2$ on the multiple VSD rearrangements that could be resolved

from the fluorescent report of Q208C*. We found that, in contrast to the large effect seen in wild type (Fig. 5c), the rapamycin induced depletion of $PI(4,5)P_2$ had almost no effect on constructs containing any of the individual linker mutations (Fig. 5f, Supp. Fig. 12b, c, Supp. Table 3).

Thus, $PI(4,5)P_2$ and the basic residues in the VSD-PD linker appear to regulate the same late step of VSD motion and single linker neutralization mutations are sufficient to greatly blunt the modulation by $PI(4,5)P_2$. Together, these findings suggest that $PI(4,5)P_2$ acts through the linker.

## Discussion

We have probed the interplay between the voltage-driven conformational changes in the VSD of Ci-VSP and the functional state of its PD. We assessed combined catalytic site and inter-domain linker mutations to examine enzyme activity of the full-length protein in live cell membranes and of the isolated PD *in vitro*. We also investigated the structural rearrangements of the VSD of the intact protein measured by Voltage Clamp Fluorometry. The results identify a rearrangement that depends on both the $PI(4,5)P_2$ substrate and on conserved basic residues in the inter-domain linker.

Previous studies showed that the inter-domain linker is critical for the voltage dependent activity of the full-length protein, with a particular importance of several basic residues at the phosphatase (C-terminal) end of the linker1,15. We found that three basic residues examined individually, K252, R253 and R254 are essential for catalysis in the living cell, with neutralization mutations leaving no detectable voltage dependent activity in K252Q and R254Q and drastically reducing activity in R253Q. We asked whether this loss of activity is due to an effect on inter-domain coupling or to a direct effect on the enzyme. We found K252Q and R254Q have reduced activity in the isolated linker-PD fragment *in vitro*. While the reduction in activity of the linker-PD construct *in vitro* was less extreme than what was seen for the full-length protein in live cells, the direct effect of K252Q and R254Q on the function of the phosphatase prevent a clear cut conclusion about their possible role in coupling. In contrast, R253Q had normal activity in the linker-PD construct *in vitro*, but ~80% reduced activity in the full-length protein in cells, consistent with an effect on coupling.

To clarify the role of the linker in inter-domain coupling, we developed a second assay that measures the coupling in the opposite direction. Rather than measuring the effect of voltage-driven VSD rearrangements on phosphatase activity, we measured the effect of mutations in the phosphatase catalytic site on VSD motion. This approach had the added advantage of a direct, high signal to noise and time-resolved measure of VSD conformation using VCF. We found that linker neutralizations reduced or eliminated the influence of catalytic site mutations on VSD motion. K252Q ablated the PD to VSD influence and completely eliminated voltage dependent activity. R253Q, on the other hand, caused a substantial but incomplete reduction in the influence of the PD mutants on the VSD and largely, but incompletely, reduced voltage dependent activity. Together, the findings show that the conserved basic residues in the VSD-PD linker play a central role in inter-domain coupling.

We wondered how the linker could alter the functional state of the enzyme in response to voltage sensing motions of the VSD. We obtained an insight into this when we found that deletion of the linker from the isolated PD abolishes activity *in vitro*. This suggests that the linker acts as a positive regulator of the enzyme. Moreover, it suggests that the mechanism of coupling is that the voltage-driven rearrangement of the VSD changes the conformation of the linker from an inactive form at negative voltage into an active form, which turns the enzyme on at positive voltage (Fig. 6).

The homologue of the Ci-VSP linker is the N-terminus of PTEN, which has been shown to bind to $PI(4,5)P_2$ through the same basic residues that we examined here in Ci-VSP11–14,30,31. A recent study on Ci-VSP proposed that $PI(4,5)P_2$ also binds to the Ci-VSP linker12. If this were the case then, given the role we documented for the linker in inter-domain coupling, we would expect that $PI(4,5)P_2$ might have an effect on Ci-VSP gating. Indeed, we found that $PI(4,5)P_2$ modulates a specific step of VSD motion: a late step that takes place at positive voltage. The same late VSD rearrangement was selectively affected by mutation of the linker's basic residues. Our findings suggest that $PI(4,5)P_2$ binding stabilizes the linker in its activating state. This effect may be explained by $PI(4,5)P_2$ binding to the basic residues, however direct evidence will be required to prove such an interaction.

The finding that the substrate of the enzyme is also a modulator implies that Ci-VSP could function as a feedback system. We propose a model in which the linker is primed and that the VSD and phosphatase are coupled when $PI(4,5)P_2$ levels are high, thus enabling membrane depolarization to turn on phosphatase activity (Fig. 6). As the enzymatic activity of Ci-VSP progresses and $PI(4,5)P_2$ levels decrease, we propose that the linker loses its $PI(4,5)P_2$ and that the enzyme is consequently uncoupled from the VSD, thereby terminating activity. Such modulation by substrate could enhance catalysis when $PI(4,5)P_2$ is high and lower activity when $PI(4,5)P_2$ is low to prevent excessive depletion.

## Materials and Methods

### Molecular Biology

The Ci-VSP in the pSD64TF vector was kindly provided by Dr. Y. Okamura (Osaka University, Osaka, Japan). The cytosolic phosphatase Ci-VSP DNA (encoding amino acids 240–576 or 256–576) was sub-cloned into the *NdeI* and *Hin*dIII sites of the pET-28b vector for bacterial expression. The LDR and CFInp constructs were kindly provided by Dr. T. Meyer (Stanford University, Palo Alto, CA) and subcloned into pGEMHE vectors. The IRK1 construct was kindly provided by Dr. E. Reuveny (Weizmann Institute of Science, Rehovot, Israel). The mGluR1α construct was kindly provided by S. Nakanishi (Osaka Bioscience Institute, Osaka, Japan). All point mutations were made using QuikChange (Stratagene). All DNA was confirmed by DNA sequencing. RNA was transcribed using either T7, T3 or SP6 mMessage mMachine (Ambion) kits.

### Voltage Clamp Fluorometry

Voltage clamp fluorometry was performed as described previously17. Briefly, *Xenopus laevis* oocytes were injected with 50 nl mRNA at 0.02–1.2 μg/μl depending on the

experiment. Different RNA ratios were used for different co-injection experiments: a 40:1 ratio for experiments co-expressing Ci-VSP and 5HT2C receptors (total RNA ~0.8 μg/μl), a 3:1 ratio for experiments co-expressing Ci-VSP and mGluR1α receptors (total RNA ~0.7 μg/μl), and either a 4:1:1 or a 2:1:1 ratio for experiments co-expressing Ci-VSP, LDR, and CFInp (either wild type or D281A, total RNA ~0.8–1.2 μg/μl). Cells were then incubated in ND-96 (96 mM NaCl, 2 mM KCl, 1.8 mM $CaCl_2$, 1 mM $MgCl_2$, 50 mg/ml gentamicin, 2.5 mM Na pyruvate and 5 mM HEPES, pH 7.6) at 18°C for 24–48 hours. Injected oocytes were treated with a 1 mM solution of glycine maleimide32 to block native cysteines before protein expression. A Nikon Diaphot inverted microscope with a 20× 0.75 NA fluorescence objective (Nikon) was used with a Dagan CA-1 amplifier (Dagan Corporation), illuminated with a 150 W xenon lamp and intensity was measured with a Hamamatsu HC120-05 photomultiplier tube. The amplifier, photomultiplier and Uniblitz shutter (Vincent Associates) were controlled by the Digidata-1440 board and pClamp10 software package (Axon Instruments). Light was filtered through an HQ535/50 excitation filter, an HQ610/75 emission filter and a Q565LP dichroic (Chroma Technology). Fluorescence signals were low pass filtered at 2 kHz through an eight-pole Bessel filter (Frequency Devices).

On the day of the experiment, cells were incubated in a high potassium solution (92 mM KCl, 0.75 mM $CaCl_2$, 1 mM $MgCl_2$, 10 mM HEPES, pH7.5) with 12 μM tetramethylrhodamine-6-maleimide (Invitrogen) for one hour on ice and in the dark. After extensive washing with ND-96, the cells were stored in ND-96, in the dark and at 12°C until the time of the experiment. Recording solutions were either ND-96' (without the gentamicin or pyruvate) or NMG buffer (110 mM N-methyl-D-glucamine (NMG) methanesulfonic acid (MS), 2 mM KMS, 2 mM $Ca(MS)_2$, 10 mM HEPES, pH 7.5) to limit leak currents. In all experiments only cells with a good control of voltage were analyzed and reported voltages and voltage steps were actual measurements.

Cells were constantly perfused with ND-96' for co-injection experiments. For experiments with 5HT2C, an initial F-V protocol (t=0, voltage jumps from −150 mV to 200 mV in 10 mV increments) was followed by perfusion of 5–10 μM serotonin (Sigma) for 10–40 s. The resulting $Ca^{2+}$ activated $Cl^-$ currents were monitored to confirm expression of the 5HT2C receptor. Then at t=5 minutes, a final F-V protocol was recorded. A similar protocol was used for experiments with mGluR1α, adding 100 μM glutamate. For experiments with LDR and CFInp, the initial F-V protocol (t=0) was followed by perfusion of 0.5–1 μM rapamycin (Sigma) for 3–5 minutes then by ND-96' until the final F-V protocol at t=10 minutes.

### Electrophysiological measure of activity

Ci-VSP catalytic activity was measured indirectly by detecting $PI(4,5)P_2$ via its activation of the inwardly-rectifying IRK1 R228Q $K^+$ channel (IRK1Q) as described previously17. The R228Q mutation of IRK1 was used to alter the sensitivity of the channel for $PI(4,5)P_2$ into an observable range. A brief description of the protocol is as follows: the cell was depolarized to 60 mV to turn Ci-VSP on until a steady state current was established (~100 s). Then the cell was hyperpolarized to −100 mV to turn Ci-VSP off until a steady state was re-established (~400 s) (Supp. Fig. 2). The resulting change in current between the on and off states of Ci-VSP was measured and expressed as percent activity. Currents were leak

subtracted by assuming a voltage-independent linear leak. Current was measured at −100 mV after the test holding potential and leak was measured at +50 mV where the IRK channels should be blocked by $Mg^{2+}$ and polyamines and the following equation applied to calculate the leak subtracted (LS) current: $I_{ls} = I_{-100mV} + 2I_{+50mV}$. The percent activity was calculated as: $\Delta I/I_{max} = (I_{-100mV\ last} - I_{+60mV\ last})/ I_{-100mV\ last}$. A similar protocol was used to test for $PI(4,5)P_2$ depletion via activation of the 5HT2C receptor, with IRK1Q serving as the $PI(4,5)P_2$ reporter.

For these experiments, 50 nl of mRNA was injected into *Xenopus laevis* oocytes. Different RNA ratios were used for the different experiments: a 10:1 ratio for experiments co-expressing Ci-VSP and IRK1Q (total RNA ~0.9 μg/μl), a 4:1 ratio for experiments co-expressing IRK1Q and 5HT2C receptor (total RNA ~0.1 μg/μl) and a 2:2:1 ratio for experiments co-expressing LDR, CFInp and IRK1Q (total RNA ~0.5 μg/μl). Cells were incubated in ND-96 at 18°C for 16–48 hours. The recording solutions contained 90 mM KMS, 3 mM $Mg(MS)_2$, 8 mM KOH, 10 mM HEPES, pH 7.4. Other conditions were the same as for voltage clamp fluorometry.

### Data Analysis

Kinetic and steady-state traces were analyzed using Igor Pro and Microsoft Excel software. Kinetic traces were fit with double exponential equations. Steady-state voltage dependent traces were fit with Boltzmann equations. Data were normalized to the amplitude of the Boltzmann fits and the error bars indicate the standard error of the mean. Statistical significance was determined using the student's t test. Confocal images were analyzed using MatLab software.

## Supplementary Material

Refer to Web version on PubMed Central for supplementary material.

## Acknowledgments

This work was supported by grants R01NS035549 (E.Y.I.), U24NS57631 (E.Y.I), and R01DC007664 (D.L.M.) from the US National Institutes of Health and an American Heart Association Established Investigator Award (D.L.M). We thank Y. Okamura (Japanese National Institute for Physiological Sciences) for kindly providing the Ci-VSP cDNA, T. Meyer (Stanford University) for kindly providing the LDR and CFInp cDNA, E. Reuveny (Weizmann Institute of Science, Rehovot, Israel) for providing the IRK1 construct, S. Nakanishi (Osaka Bioscience Institute, Osaka, Japan) for providing the mGluR1α receptor, J. Groves and P. Nair (University of California, Berkeley) for access to and instructions on use of the lipid extruder and H. Janovjak, K. Nakajo, E. Peled and F. Tombola for helpful discussion.

## References

1. Murata Y, Iwasaki H, Sasaki M, Inaba K, Okamura Y. Phosphoinositide phosphatase activity coupled to an intrinsic voltage sensor. Nature. 2005; 435:1239–1243. [PubMed: 15902207]
2. Okamura Y, Murata Y, Iwasaki H. Voltage-sensing phosphatase: actions and potentials. J Physiol. 2009; 587:513–520. [PubMed: 19074969]
3. Worby CA, Dixon JE. Phosphoinositide phosphatases: emerging roles as voltage sensors? Mol Interv. 2005; 5:274–277. [PubMed: 16249522]
4. Lu Z, Klem AM, Ramu Y. Ion conduction pore is conserved among potassium channels. Nature. 2001; 413:809–813. [PubMed: 11677598]

5. Lu Z, Klem AM, Ramu Y. Coupling between voltage sensors and activation gate in voltage-gated K + channels. J Gen Physiol. 2002; 120:663–676. [PubMed: 12407078]
6. Long SB, Campbell EB, Mackinnon R. Crystal structure of a mammalian voltage-dependent Shaker family K+ channel. Science. 2005; 309:897–903. [PubMed: 16002581]
7. Murata Y, Okamura Y. Depolarization activates the phosphoinositide phosphatase Ci-VSP, as detected in Xenopus oocytes coexpressing sensors of PIP2. J Physiol. 2007; 583:875–889. [PubMed: 17615106]
8. Iwasaki H, et al. A voltage-sensing phosphatase, Ci-VSP, which shares sequence identity with PTEN, dephosphorylates phosphatidylinositol 4,5-bisphosphate. Proc Natl Acad Sci U S A. 2008; 105:7970–7975. [PubMed: 18524949]
9. Halaszovich CR, Schreiber DN, Oliver D. Ci-VSP is a depolarization-activated phosphatidylinositol-4,5-bisphosphate and phosphatidylinositol-3,4,5-trisphosphate 5'-phosphatase. J Biol Chem. 2009; 284:2106–2113. [PubMed: 19047057]
10. Maehama T, Taylor GS, Dixon JE. PTEN and myotubularin: novel phosphoinositide phosphatases. Annu Rev Biochem. 2001; 70:247–279. [PubMed: 11395408]
11. Iijima M, Huang YE, Luo HR, Vazquez F, Devreotes PN. Novel mechanism of PTEN regulation by its phosphatidylinositol 4,5-bisphosphate binding motif is critical for chemotaxis. J Biol Chem. 2004; 279:16606–16613. [PubMed: 14764604]
12. Walker SM, Leslie NR, Perera NM, Batty IH, Downes CP. The tumour-suppressor function of PTEN requires an N-terminal lipid-binding motif. Biochem J. 2004; 379:301–307. [PubMed: 14711368]
13. Vazquez F, et al. Tumor suppressor PTEN acts through dynamic interaction with the plasma membrane. Proc Natl Acad Sci U S A. 2006; 103:3633–3638. [PubMed: 16537447]
14. Rahdar M, et al. A phosphorylation-dependent intramolecular interaction regulates the membrane association and activity of the tumor suppressor PTEN. Proc Natl Acad Sci U S A. 2009; 106:480–485. [PubMed: 19114656]
15. Villalba-Galea CA, Miceli F, Taglialatela M, Bezanilla F. Coupling between the voltage-sensing and phosphatase domains of Ci-VSP. J Gen Physiol. 2009; 134:5–14. [PubMed: 19564425]
16. Mannuzzu LM, Moronne MM, Isacoff EY. Direct physical measure of conformational rearrangement underlying potassium channel gating. Science. 1996; 271:213–216. [PubMed: 8539623]
17. Kohout SC, Ulbrich MH, Bell SC, Isacoff EY. Subunit organization and functional transitions in Ci-VSP. Nat Struct Mol Biol. 2008; 15:106–108. [PubMed: 18084307]
18. Hossain MI, et al. Enzyme domain affects the movement of the voltage sensor in ascidian and zebrafish voltage-sensing phosphatases. J Biol Chem. 2008; 283:18248–18259. [PubMed: 18375390]
19. Villalba-Galea CA, Sandtner W, Starace DM, Bezanilla F. S4-based voltage sensors have three major conformations. Proc Natl Acad Sci U S A. 2008; 105:17600–17607. [PubMed: 18818307]
20. Steck PA, et al. Identification of a candidate tumour suppressor gene, MMAC1, at chromosome 10q23.3 that is mutated in multiple advanced cancers. Nat Genet. 1997; 15:356–362. [PubMed: 9090379]
21. Duerr EM, et al. PTEN mutations in gliomas and glioneuronal tumors. Oncogene. 1998; 16:2259–2264. [PubMed: 9619835]
22. Gronbaek K, Zeuthen J, Guldberg P, Ralfkiaer E, Hou-Jensen K. Alterations of the MMAC1/PTEN gene in lymphoid malignancies. Blood. 1998; 91:4388–4390. [PubMed: 9596690]
23. Downes CP, et al. Acute regulation of the tumour suppressor phosphatase, PTEN, by anionic lipids and reactive oxygen species. Biochem Soc Trans. 2004; 32:338–342. [PubMed: 15046604]
24. Xiao Y, et al. PTEN catalysis of phospholipid dephosphorylation reaction follows a two-step mechanism in which the conserved aspartate-92 does not function as the general acid--mechanistic analysis of a familial Cowden disease-associated PTEN mutation. Cell Signal. 2007; 19:1434–1445. [PubMed: 17324556]
25. Flint AJ, Tiganis T, Barford D, Tonks NK. Development of "substrate-trapping" mutants to identify physiological substrates of protein tyrosine phosphatases. Proc Natl Acad Sci U S A. 1997; 94:1680–1685. [PubMed: 9050838]

26. Julius D, MacDermott AB, Axel R, Jessell TM. Molecular characterization of a functional cDNA encoding the serotonin 1c receptor. Science. 1988; 241:558–564. [PubMed: 3399891]

27. Suh BC, Inoue T, Meyer T, Hille B. Rapid chemically induced changes of PtdIns(4,5)P2 gate KCNQ ion channels. Science. 2006; 314:1454–1457. [PubMed: 16990515]

28. Varnai P, Thyagarajan B, Rohacs T, Balla T. Rapidly inducible changes in phosphatidylinositol 4,5-bisphosphate levels influence multiple regulatory functions of the lipid in intact living cells. J Cell Biol. 2006; 175:377–382. [PubMed: 17088424]

29. Lukacs V, et al. Dual regulation of TRPV1 by phosphoinositides. J Neurosci. 2007; 27:7070–7080. [PubMed: 17596456]

30. Campbell RB, Liu F, Ross AH. Allosteric activation of PTEN phosphatase by phosphatidylinositol 4,5-bisphosphate. J Biol Chem. 2003; 278:33617–33620. [PubMed: 12857747]

31. Redfern RE, et al. PTEN phosphatase selectively binds phosphoinositides and undergoes structural changes. Biochemistry. 2008; 47:2162–2171. [PubMed: 18220422]

32. Borah HN, Boruah RC, Sandhu JS. Microwave-induced one-pot synthesis of N-carboxyalkyl maleimides and phthalimides. Journal of Chemical Research-S. 1998:272. +

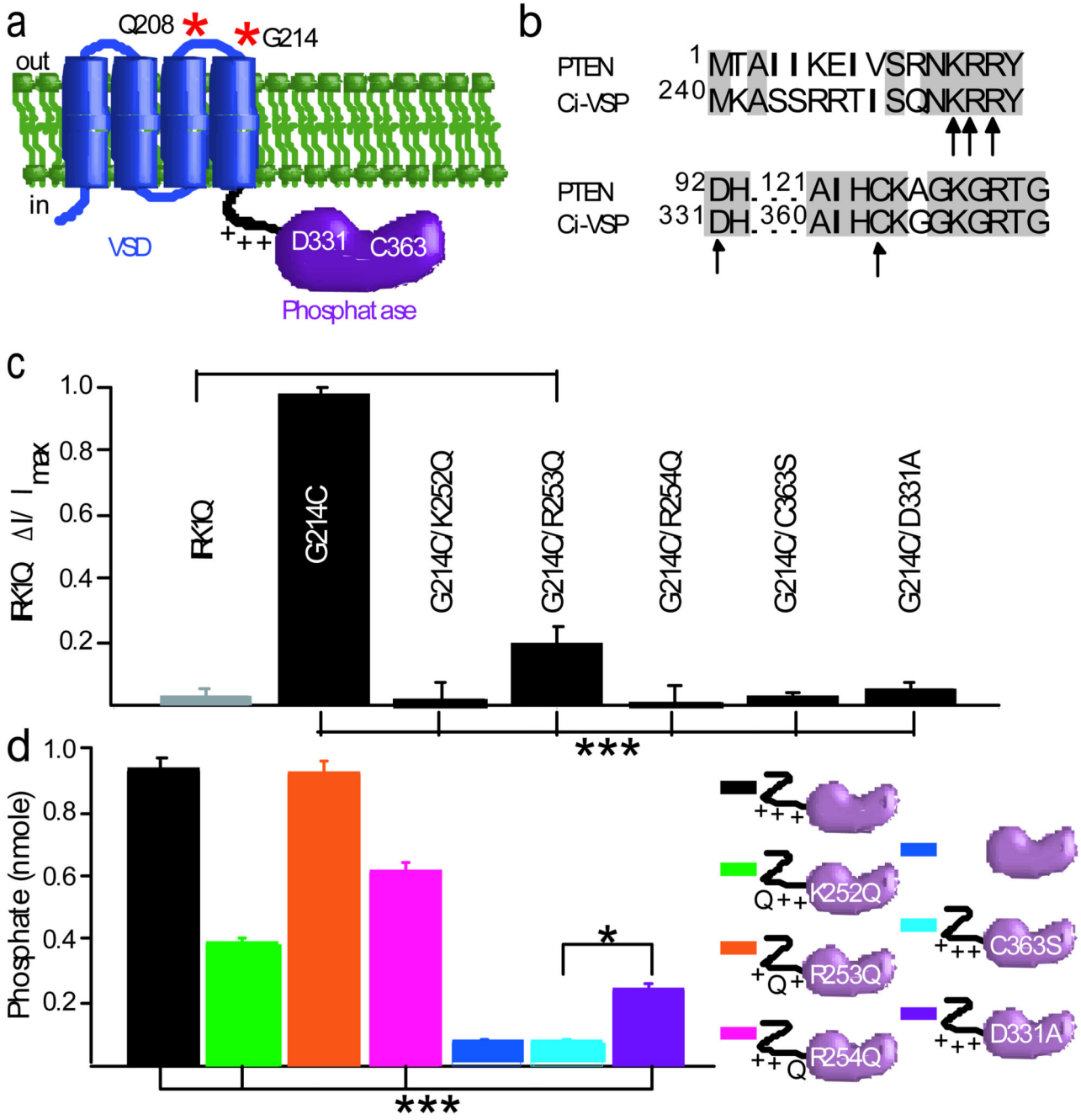


**Figure 1. Linker and catalytic site mutants reduce or abolish activity**

**a)** Cartoon of Ci-VSP domains. The VSD consists of 4 helices, S1–S4. Q208 and G214 in the S3–S4 external loop are sites of cysteine substitution and attachment of the environmentally sensitive fluorophore TMRM (red asterisks). The sixteen amino acid linker (black) connects S4 of the VSD to the PD (purple). It contains 3 conserved basic residues (+): K252, R253, R254. Two conserved catalytic site residues, D331 and C363, shown in the PD. **b)** Alignment of human PTEN with Ci-VSP: (Top) PTEN N-terminus and VSD-PD linker of Ci-VSP; (Bottom) Active site residues. Identical residues highlighted (gray),

arrows mark Ci-VSP residues mutated in this study. **c)** Activity of full-length Ci-VSP in oocytes measured from voltage dependence of IRK1Q current in cells also expressing Ci-VSP. Average data for IRK1Q alone (n=26) or IRK1Q coexpressed with G214C (n=9); G214C/K252Q (n=10); G214C/R253Q (n=8); G214C/R254Q (n=6); G214C/C363S (n=6); G214C/D331A (n=6). $\Delta I/I_{max}$ was calculated from steady-state current of active Ci-VSP (+60 mV) versus inactive Ci-VSP (−100 mV) (Materials and Methods & Supp. Fig. 2). Asterisks indicate statistically significant differences using the student's t test, p=0.008. **d**) *In vitro* malachite green activity assay with PS/PI(3,4,5)$P_3$ vesicles and the cytosolic fragment of Ci-VSP, containing amino acids 240–576, 256–576 or mutations (in linker or PD). Constructs identified in cartoons on right as in (a) with PD in light purple. All error bars are ± SEM. * = $p<0.05$; *** = $p<0.001$ for comparison of marked mutants to wildtype.

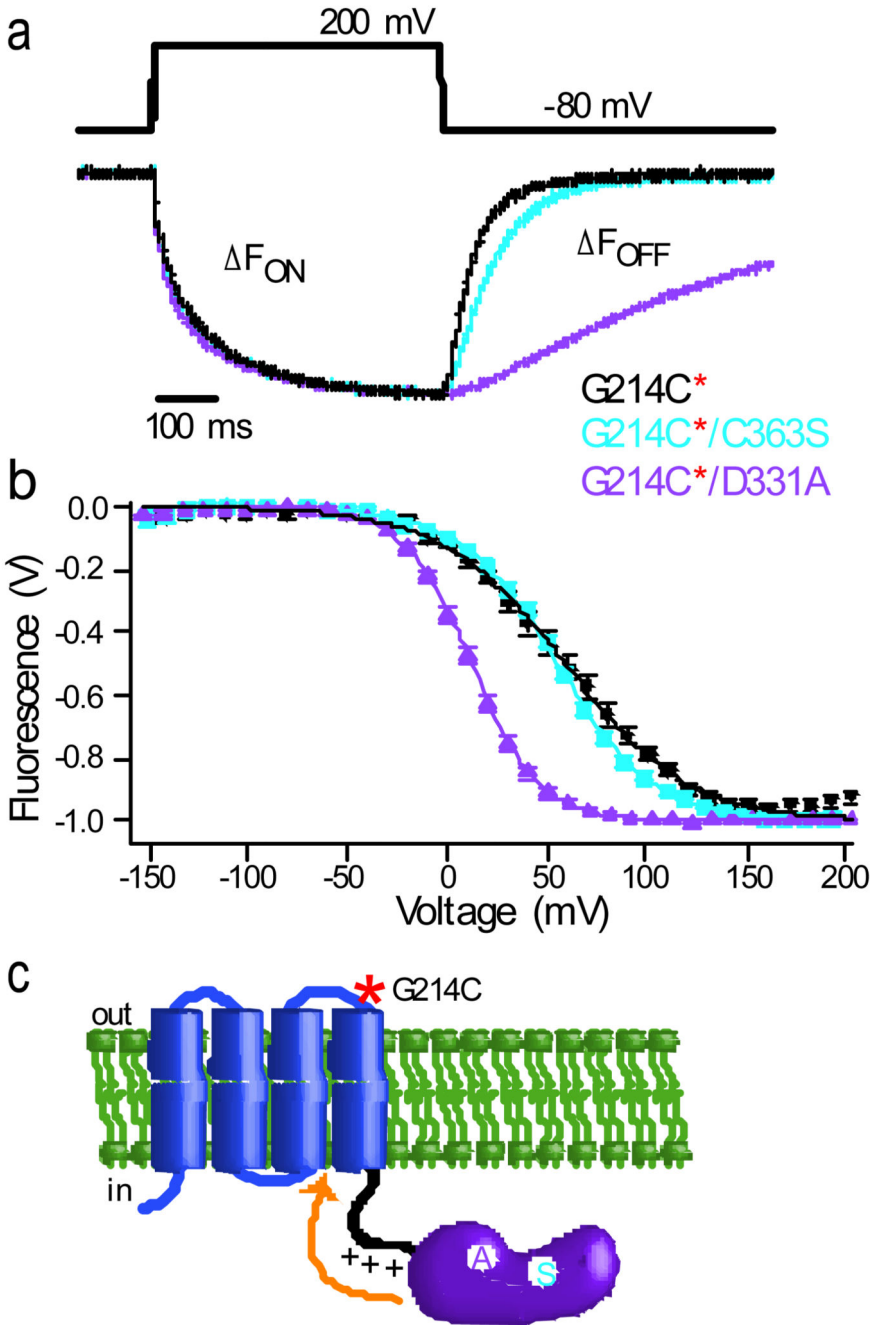


**Figure 2. Mutations of PD catalytic site alter VSD motion**

**a)** Representative fluorescence traces during a step from hp = −80 mV to +200 mV in G214C* (black), G214C*/C363S (blue) and G214C*/D331A (purple). The catalytic site mutations alter S4 $\Delta F_{ON}$ and $\Delta F_{OFF}$ motions, with more dramatic slowing of the $\Delta F_{OFF}$ motion. Traces normalized to the maximal fluorescence change. Voltage trace reports actual voltage recorded during acquisition. **b)** Normalized F-Vs. Same colors and hp as in a). Data fit to single Boltzmann equations (see Materials and Methods, Supp. Table 1). Catalytic site mutants negatively shift F-V. Error bars (mostly smaller than symbols) are ± SEM, n ≥ 9. **c)**

Cartoon depicting influence of mutations at catalytic site of PD on VSD motion detected by TMRM (asterisk) attached to G214C, at the outer end of S4.

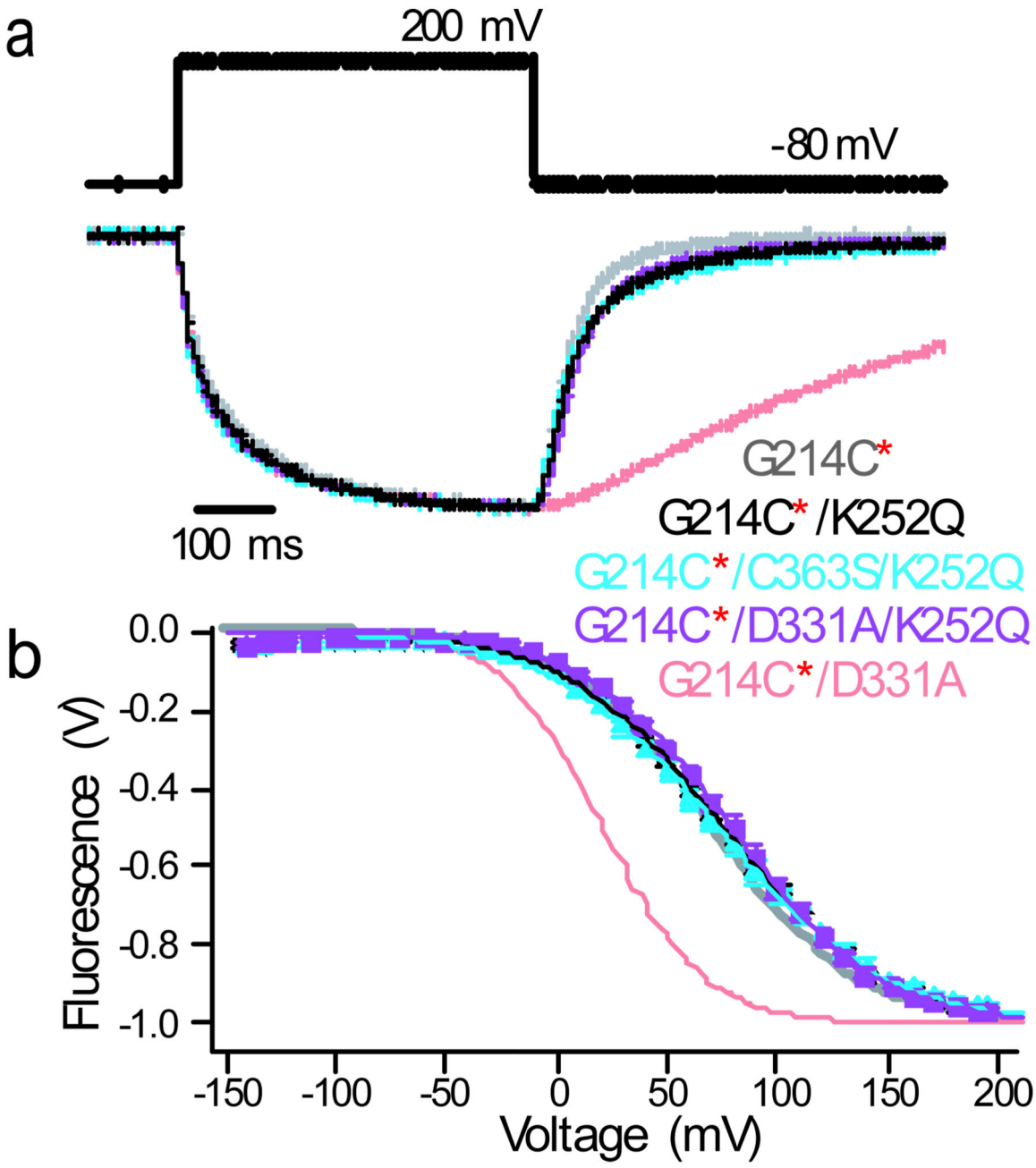


**Figure 3. Linker charge neutralization eliminates effect of catalytic site mutations on VSD motion**

**a)** Representative normalized fluorescence traces evoked by step from hp = −80 mV to +200 mV. G214C*/K252Q (black, same as in Supp. Fig 5.), G214C*/C363S/K252Q (blue), G214C*/D331A/K252Q (purple), G214C* (gray, from Fig. 2) and G214C*/D331A (pale red, from Fig. 2). **b**) F-Vs fit to single Boltzmann equation, with symbol size indicating ± SEM, n ≥ 10. Same colors and hp as in (a). K252Q eliminates both the slowing of $\Delta F_{OFF}$ (a)

and the shift of F-V (b) caused by C363S and D331A catalytic site mutations. Data fit to single Boltzmann equations (see Supp. Table 1).

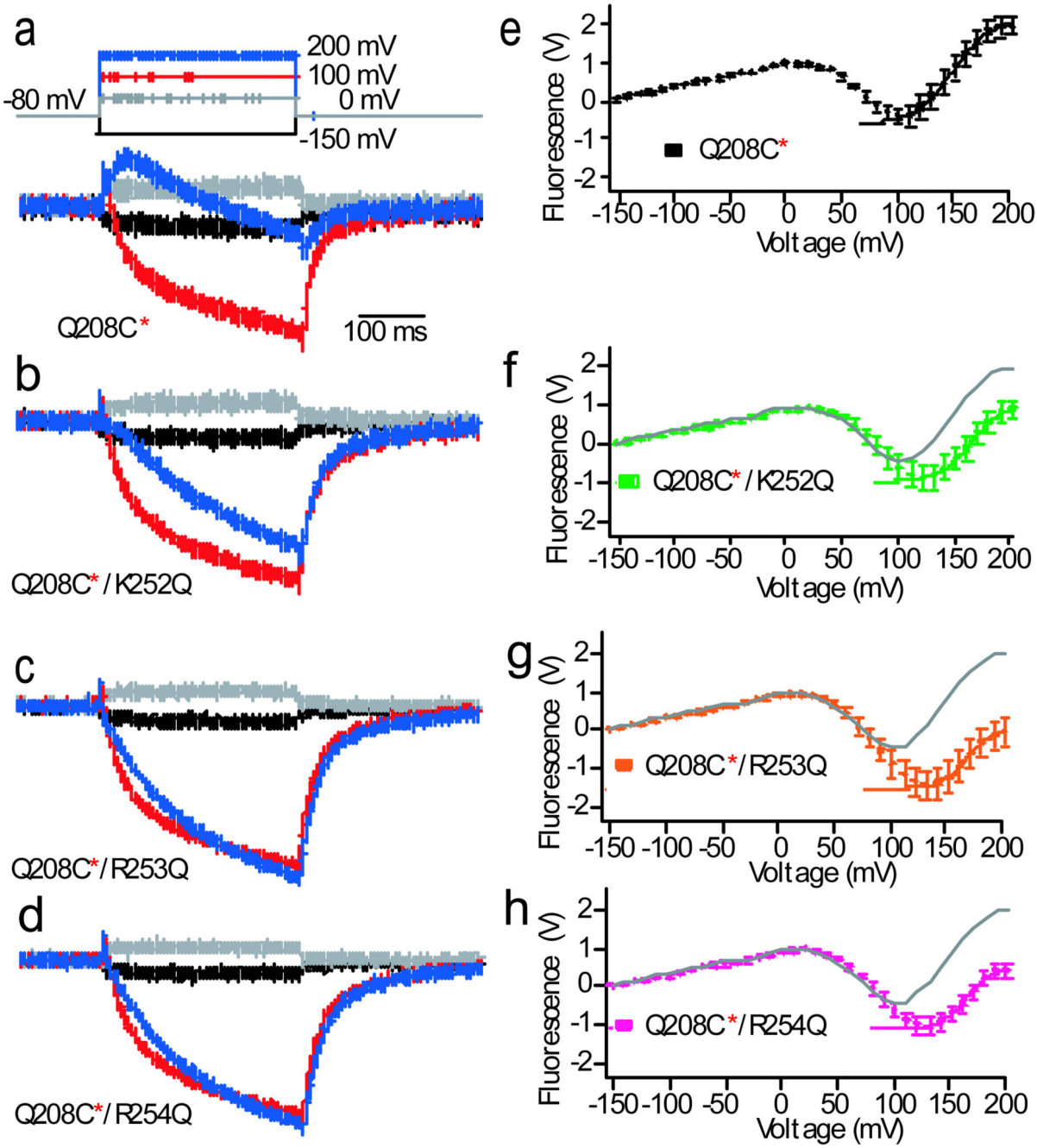


**Figure 4. Linker mutations alter late component of VSD motion**

**a–d)** Representative Q208C* fluorescence traces evoked by steps from hp= −80 mV to −150 mV (black), 0 mV (gray), +100 mV (red) and +200 mV (blue) in wild type, Q208C* (**a**) and the three linker mutations: Q208C*/K252Q (**b**), Q208C*/R253Q (**c**) and Q208C*/R254Q (**d**) **e–h**) F-V relationships measured at the peak of the second upper component for wild type (Q208C*) and the linker mutants normalized by component from −150 mV to 0 mV. Wild type (Q208C*) from (e) superimposed for comparison in (f-h) as gray line. Linker mutants diminish amplitude of late fluorescence increase component and shift its voltage

dependence to the right. Data fit to single Boltzmann equations (Supp. Table 1), error bars are ± SEM, n ≥8.

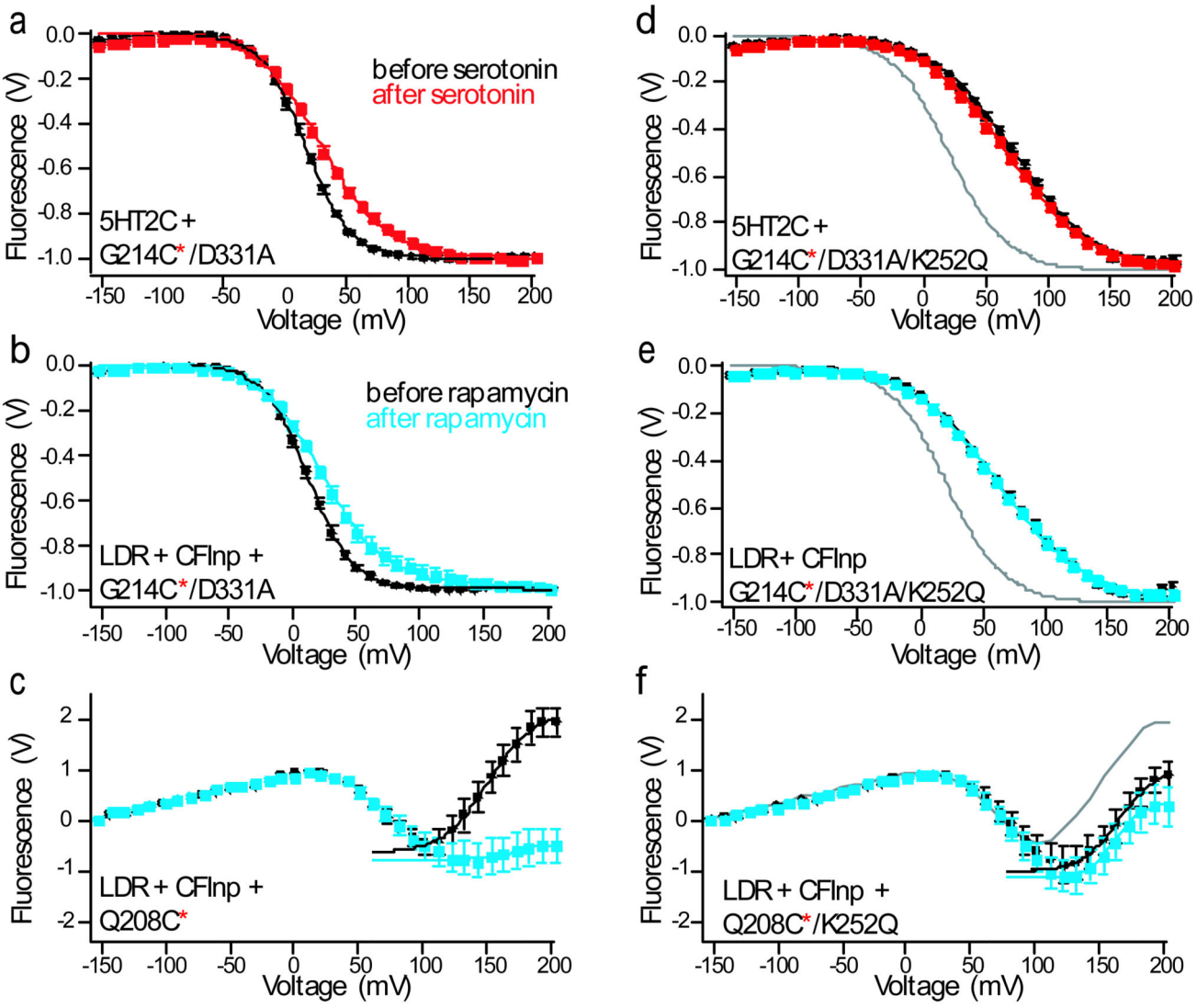


**Figure 5. PI(4,5)$P_2$ depletion alters VSD motion in manner dependent on the VSD-PD linker**

**a**) 5HT2C receptor activation by serotonin (activates conversion of PI(4,5)$P_2$ into $IP_3$ and DAG by phospholipase C) shifts the F-V of the catalytic site mutation G214C*/D331A to the right and decreases the steepness. F-Vs before (black) and 5 min after addition of 10 μM serotonin (red). **b, c**) Rapamycin-induced membrane localization of the lipid phosphatase CFInp (converts PI(4,5)$P_2$ into PI(4)P) shifts the F-V of the catalytic site mutation G214C*/D331A to the right and decreases the steepness (**b**), and decreases the amplitude and shifts to the right the late component of fluorescence increase of wild type Q208C* (**c**). F-Vs before (black) and 5–10 min after (blue) addition of 1 μM rapamycin. **d)** Catalytic site mutation, G214C*/D331A, was not affected by 5HT2C receptor activation in presence of K252Q linker mutation. F-Vs before (black) and 5 min after (red) addition of serotonin. F-V of G214C*/D331A with a wild type linker and no 5HT2C activation shown for comparison in gray. **e, f)** Rapamycin-induced PI(4,5)$P_2$ depletion by activation of CFInp has no detectable effect in G214C*/D331A/K252Q (**e**), and a small effect in the linker mutants

Q208C*/K252Q (**f**) compared to wild type Q208C* (**c**). F-Vs before (black) and 5–10 min after rapamycin (blue). (F-V of G214C*/D331A in gray for comparison in **e** and F-V of Q208C* in gray for comparison in **f**). Error bars are ± SEM, n ≥9. Data fit to single Boltzmann equations (see Supp. Table 2 & 3).

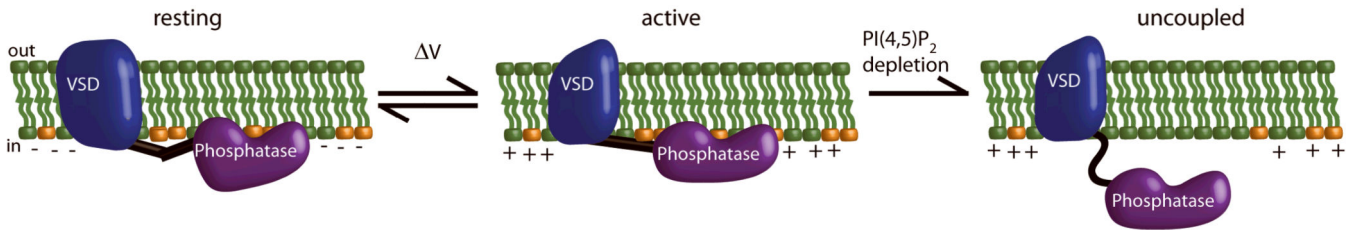


**Figure 6. Model of linker regulation and coupling in Ci-VSP**

Left) At negative voltage the VSD is in a resting state and the linker is distorted into a non-functional state. Middle) At positive voltage the VSD is in an activated conformation and the linker relaxes into the positive regulatory state that is necessary for activity of the isolated PD *in vitro*. $PI(4,5)P_2$ stabilizes the activated state, possibly by interacting with the linker. Right) The depletion of $PI(4,5)P_2$ by Ci-VSP activity leads to a destabilization of the activated state and uncoupling of the VSD from the phosphatase, thus turning the enzyme off even though the membrane is still depolarized.